Article
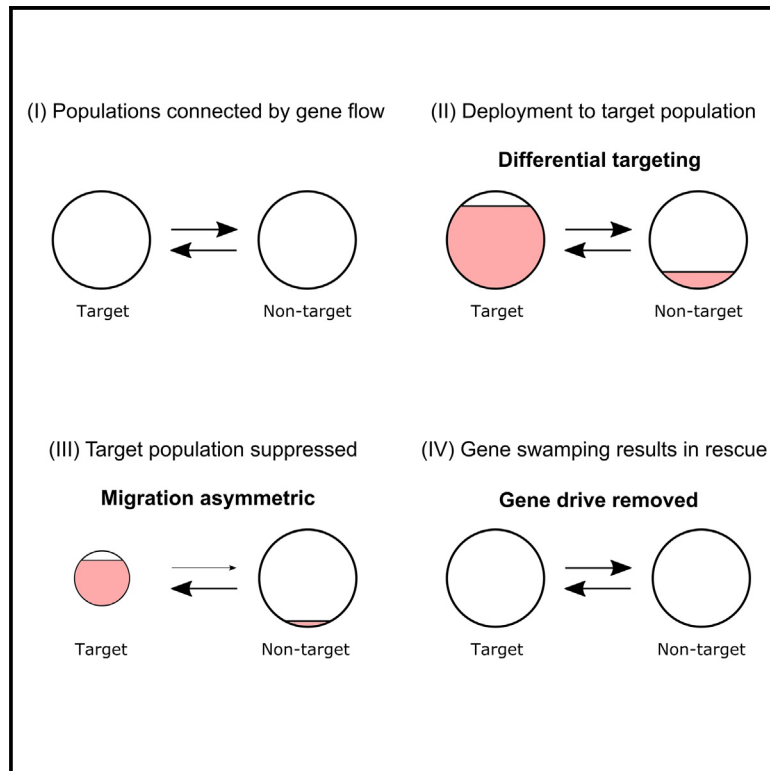
Rescue by gene swamping as a gene drive deployment strategy

Graphical abstract

Authors

Keith D. Harris, Gili Greenbaum

Correspondence

keith.harris@mail.huji.ac.il (K.D.H.),
gil.g@mail.huji.ac.il (G.G.)

In brief

Gene drives carry the risk of unintended spread to non-target populations and species. Harris et al. develop a model that demonstrates a potential fail-safe for deployment, identifying gene drive designs that are expected to generate a short-term suppression window followed by removal of the gene drive from the system.

Highlights

- Gene swamping can slow or even reverse the spread of gene drives

- We developed a gene drive model incorporating an evolutionary-demographic feedback

- We identified a deployment outcome of short-term suppression followed by removal

- This outcome can prevent spillover and is robust to the evolution of resistance

CellPress

Article

Rescue by gene swamping as a gene drive deployment strategy

Keith D. Harris[1,*] and Gili Greenbaum[1,2,*]

[1]Department of Ecology, Evolution and Behavior, The Hebrew University of Jerusalem, Jerusalem 91904, Israel
[2]Lead contact
*Correspondence: keith.harris@mail.huji.ac.il (K.D.H.), gil.g@mail.huji.ac.il (G.G.)
https://doi.org/10.1016/j.celrep.2023.113499

SUMMARY

Gene drives are genetic constructs that can spread deleterious alleles with potential application to population suppression of harmful species. As gene drives can potentially spill over to other populations or species, control measures and fail-safe strategies must be considered. Gene drives can generate a rapid change in the population's genetic composition, leading to substantial demographic decline, processes that are expected to occur at a similar timescale during gene drive spread. We developed a gene drive model that combines evolutionary and demographic dynamics in a two-population setting. The model demonstrates how feedback between these dynamics generates additional outcomes to those generated by the evolutionary dynamics alone. We identify an outcome of particular interest where short-term suppression of the target population is followed by gene swamping and loss of the gene drive. This outcome can prevent spillover and is robust to the evolution of resistance, suggesting it may be suitable as a fail-safe strategy for gene drive deployment.

INTRODUCTION

Gene drives are genetic constructs that allow the spread of deleterious alleles by violating Mendelian inheritance patterns.[1] With CRISPR-Cas9-based technology, gene drives can potentially be used to suppress or eliminate wild populations,[2,3] and they have the potential for revolutionizing biocontrol.[4] However, there are substantial concerns that need to be addressed before deployment in the wild can be considered, including the spillover of the gene drive to other populations or species[5,6] and the evolution of resistance to the gene drive.[7] Addressing these concerns is complicated by the possible interaction between the evolutionary dynamics of the spread of the gene drive in the population and its demographic impacts. In potential gene drive deployments, due to the rapid spread of the gene drive allele, evolutionary and demographic effects are expected to occur at similar timescales[8]; feedback between these processes may substantially shape the outcome.[9] Therefore, in order to inform gene drive design and to develop novel strategies for mitigating the risks of gene drive deployments, investigating the evolutionary-demographic dynamics of gene drives is crucial.

Mathematical and computational modeling has been instrumental in guiding gene drive research, allowing the study of key aspects in the behavior of gene drives prior to their deployment.[10,11] Population genetic models investigating the evolutionary dynamics of non-Mendelian inheritance were developed decades before the recent development of CRISPR-based drives,[12,13] and they were subsequently adjusted to more specifically model CRISPR-based gene drives.[14,15] Some models focus on whether gene drives could effectively spread in a single population,[13–15] while others focus on spread of the gene drive between discrete populations[6,16] or across a continuous landscape.[9,17,18] These models showed that, in cases in which the gene drive spreads in a population or region regardless of its initial frequency, it will spill over to all other connected populations or regions. This risk can be mitigated by designing gene drives that are specific to the genetics of the target population[19] or by using more complex genetic architectures that have slower spread dynamics such as daisy-chain drives[20] or split drives.[21,22] Without such elaborations of the gene drive construct, only with threshold-dependent gene drives (i.e., cases where the gene drive spreads only when its frequency is above a critical threshold) are spillovers potentially avoidable. Modeling efforts have also been directed to studying the evolution or resistance to the gene drive constructs,[23] showing that in some cases, resistance alleles are expected to spread rapidly in a population once they appear,[24] leading to the loss of the gene drive allele and increasing the chance of future deployments failing.

The consequence of feedback from the demographic changes caused by the gene drive on the evolutionary dynamics has been studied in continuous-space models and has been shown to affect the outcome of gene drive deployment.[9,25] In these models, the decrease in local density caused by the negative demographic effect of the gene drive allele can prevent the gene drive from spreading or lead to long-term persistence of the gene drive, with fluctuations of both the gene drive allele frequency and local population density. While these models demonstrate that demography can crucially affect the success of deployment in a continuous-space setting, where only a single region is considered, it is unclear how demographic feedback

would affect the spillover of the gene drive from the target population to other, non-target, populations. In particular, demographic changes could lead to asymmetrical gene flow between the target population and neighboring populations, thus substantially altering the risk of spillover.[6]

In order to study how the interaction between the evolutionary and demographic processes involved in gene drive spread influences deployment outcomes, we developed a model that tracks interconnected evolutionary and demographic dynamics. For tractability, the model is set in a two-population system, which allows for spillovers from the target population to the non-target population, as well as for potential gene swamping of the target population by wild-type alleles from the non-target population. Our investigation is specifically focused on identifying emerging outcomes that could be used to develop strategies that can mitigate the risks of gene drive spillovers and reduce the probability of resistance evolution.

RESULTS

The effect of demographic-evolutionary feedback on outcomes

Figure S1 and Note S1 in Data S1 detail the life cycle used for the model and provide a schematic overview of the model equations. For the full development of the model, see the method details section below.

To understand how demography influences the outcome of gene drive deployment, it is insightful to compare the outcomes of our model to that of a previous model taking into account only evolutionary dynamics.[6] This is facilitated by the parameter d in our model, which defines the degree to which the gene drive affects demography. We can consider purely evolutionary dynamics by setting $d = 0$ in our model (Figure S2A). In the purely evolutionary model, three types of qualitatively different outcomes are expected following deployment in the target population: (1) the gene drive deployment fails and the gene drive allele is lost from both populations ("*failure*"); (2) the gene drive spills over from the target population to the non-target population and is driven to fixation in both ("*spillover*"); or (3) the gene drive remains in a stable state (high frequency in the target population and low frequency in the non-target population) for low migration rates ("*differential targeting*"), but spillover or failure occur for higher migration rates. The outcome of deployment is determined by the gene drive configuration parameters (s, c, and h); for gene drive designs that are threshold dependent (in a single-population model), it is also determined by the migration rate, m.

At higher values of d, the growth rate of gene drive homozygotes, $r_{(s)}$, is correlated with s (Figure S2A), and consequently, the evolutionary dynamics of the gene drive can affect population sizes, as well as the migration rates. Because we were interested in outcomes that involve demographic effects, and feedback between the evolutionary and demographic dynamics, for all analyses, we used a value of $d = 10$ unless otherwise stated (Table S1). This is above the threshold at which the gene drive can have a demographic effect (i.e., $r_{(s)} < 1$) but not $d \rightarrow \infty$ for which $r_{(s)} \rightarrow 1 - s$. With this d value (and any $d > 0$), manipulating s also affects the growth rate of a population in which the gene

drive allele is present, and it may allow for the collapse of this population if the gene drive reaches a high enough frequency. Through characterization of the dynamics under different parameterizations of our model, we observe that incorporating demographic effects of the gene drive generates additional types of outcomes (Figure 1), and we observe a shift from the outcomes of the purely evolutionary model with increasing values of d (Figure S2B). We classified the types of outcomes according to the gene drive allele frequency and the demographic changes in the populations after 100 generations (Table S2).

Two of the outcomes, "*spillover* & *collapse*," where "*spillover*" to the non-target population is followed by "*collapse*" of both populations (Figure 1A), and "*failure*" (Figure 1E) have no targeted demographic effect and therefore represent undesirable scenarios if the goal is to contain deployment to a specific target population. However, we identified three outcomes in which differential targeting of the gene drive results in distinct demographic and long-term genetic effects. The first is long-term "*differential targeting*" and demographic "*suppression*" by the gene drive in the target population (Figure 1B). Here, fluctuations of the evolutionary and demographic dynamics eventually stabilize, and the system converges to a differential targeting state, as observed in purely evolutionary models that do not incorporate demography. With the other parameters remaining fixed, increasing the relative fitness cost of the gene drive s (with $d = 10$, this also decreases $r_{(s)}$) results in a different outcome, in which the "*oscillations*" of the evolutionary and demographic dynamics do not converge, and no steady state is reached (Figure 1C). In each cycle, a high gene drive allele frequency in the target population leads to demographic impact and a decrease in population size, as in the suppression outcome. However, consequently, gene flow from the non-target population, which now becomes proportionately larger, has an increased impact on the target population. Because this gene flow is mainly of wild-type alleles (gene drive frequencies in the non-target population are low at the differential targeting state), the gene drive allele frequency in the target population is reduced. The wild-type-abundant gene flow reduces the demographic impact of the gene drive, and the target population switches from negative to positive growth. The impact of gene flow from the non-target population is then reduced as the target population increases in size, and the gene drive again spreads to high frequencies in the target population, ending the cycle, and a new oscillation begins.

Increasing the relative fitness cost of the gene drive further can generate an additional type of outcome (Figure 1D), in which gene flow from the non-target population, coupled with negative selection against the gene drive allele, is sufficiently strong to completely remove the gene drive allele from the target population, resulting in "*gene swamping*"[26]—complete removal of the gene drive allele—followed by full demographic recovery of the target population (Figure 1F). In this outcome, unlike in any of the other outcomes, the gene drive allele is not expected to remain in any of the populations, while it still generates a significant demographic impact on the target population and only on the target population. This demographic effect is not persistent as in the suppression outcome (Figure 1B), but instead, it generates a short-term suppression phase that is expected to dissipate. Nevertheless, if other population control measures
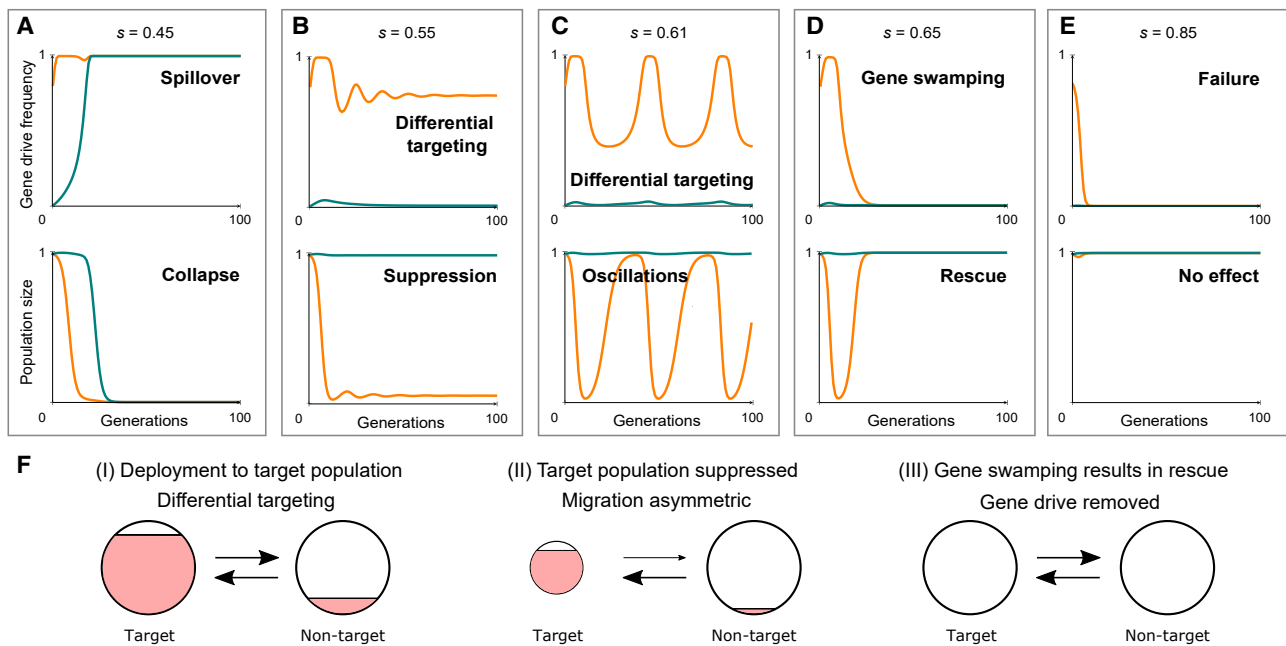
Figure 1. Distinct outcomes of deployment in a gene drive model incorporating feedback between evolution and demography

(A–E) Outcomes classified as indicated in Table S2. The top panels in (A)–(E) show the evolutionary dynamics in terms of the gene drive allele frequency, while the bottom panels show demographic dynamics in terms of the population sizes. Dynamics in the target population are shown in orange and in the non-target population in blue. (A) Gene drive spillover followed by collapse of both populations. (B) Differential targeting with stable suppression of only the target population. (C) Oscillations in the evolutionary and demographic dynamics. (D) Suppression of the target population followed by gene swamping and global removal of the gene drive. (E) Failure of the gene drive with no demographic effect. The outcomes differ only in the relative fitness cost of the gene drive, s, noted above each panel, and they are identical in all other parameters: $c = 1$, $h = 1$, $m = 0.01$, $q_1(0) = 0.8$, $d = 10$, and $r_0 = 2$.

(F) Schematic illustration of the dynamics in the gene swamping outcome in (D): (I) the gene drive is initially deployed to the target population and has a low frequency in the non-target population (gene drive allele frequency illustrated as the filled red portion); (II) as the target population is suppressed, migration becomes increasingly asymmetric, with decreased gene flow out of and increased gene flow into the target population; (III) gene swamping due to asymmetric migration leads to gene swamping and removal of the gene drive from both populations. For outcome definitions, see Table S2.

are introduced during the suppression phase, long-term suppression or elimination of the target population may be achieved. Therefore, to achieve control of the target population, this strategy would require additional types of population controls to augment genetic suppression. While the same measures could be used to augment suppression in the suppression and oscillations outcomes, in the case that these measures fail, the gene swamping outcome will have a lower risk of permanent genetic impact on the population and, consequently, of the evolution of resistance to the gene drive, because the expected final outcome is removal of the gene drive allele from the entire system (see gene swamping is robust to the evolution of resistance below).

Migration rates, gene drive configurations, and initial frequencies

To understand the relation between gene drive designs, ecological constraints, and the deployment outcomes we identified, we investigated model outcomes for different gene drive configurations (values of s, c, and h) and migration rates, m (Figure 2). For each migration rate value m, we also computed the proportion of the parameter space that each outcome occupies (for fixed h values, for tractability), in order to understand how difficult it would be to generate gene drive designs that can ensure a desired outcome (Figure 2B).

For low migration rates ($m = 10^{-6}$, denoted as $m \rightarrow 0$; left panels in Figure 2A), much of the parameter space results in failure or spillover & collapse, while, for some parameters, differential targeting, suppression, or gene swamping outcomes can be achieved (particularly for higher h values). At higher migration rates ($m = 0.01$ and $m = 0.05$), an increased range of gene drive configurations results in spillover and collapse of both populations (orange curve in Figure 2B). Importantly, while suppression outcomes (green in Figure 2) quickly become almost unachievable as migration rates increase (i.e., this outcome occupies only a narrow range in the parameter space), the gene swamping outcome (blue in Figure 2) still occupies a significant portion of the parameter range. Therefore, although the possibility of achieving gene swamping is also dependent on migration, it is achievable for higher migration rates compared to the suppression outcome (Figure 2). These results are qualitatively robust when compared to a different formulation of $r_{(s)}$ and a different population growth model (see Notes S2 and S3 in Data S1 and Figures S3–S4). With zygotic conversion, the same outcomes are identified, but spillover can be avoided for lower values of h (see Note S4 in Data S1 and Figures S5–S6).

In Figures 1 and 2, we assumed a relatively high initial gene drive allele frequency in the target population ($q_1(0) = 0.8$), meaning that four times the initial population in individuals homozygous for the gene drive allele are released. This allows us to study the
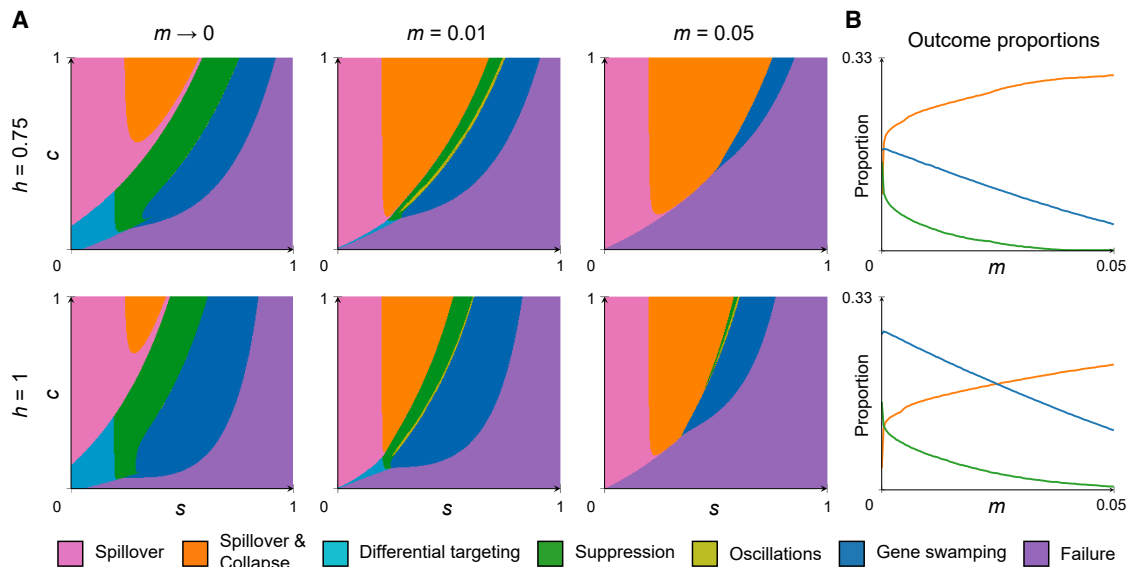
Figure 2. Model outcomes in relation to gene drive design and migration rates

Colors indicate the outcome as follows: "spillover"—spillover without collapse in pink; "spillover & collapse"—spillover and collapse of both populations due to spillover in orange; "differential targeting"—differential targeting of the gene drive without demographic effects in cyan; "suppression"—suppression of target population in green; "oscillations"—oscillations of dynamics in the target population in teal; "gene swamping"—gene swamping and subsequent rescue of the target population with loss of the gene drive in blue; "failure"—failure of the deployment (no demographic effect) and loss of the gene drive from both populations in purple.

(A) Each panel shows the outcome attained in our model for a fixed h value, for several m values, and for all s and c values.

(B) Relative proportions for spillover & collapse (orange), suppression (green), and gene swamping (blue) outcomes. Increasing migration rates increase the proportion of spillover outcomes but disproportionately affect suppression outcomes. In all panels, the parameters $q_1(0) = 0.8$, $d = 10$, and $r_0 = 2$ were used. For outcome definitions, see Table S2.

full scope of deployment outcomes that are achievable without considering limitations of the initial frequency of the gene drive. In addition, this initial frequency is comparable with some other applied population control strategies.[27] However, as this may be difficult in some organisms and scenarios, to assess the degree to which the outcomes we identified rely on this high initial frequency, we analyzed the proportion of three outcomes (spillover & collapse in orange, suppression in green, and gene swamping in blue) for different designs and migration rates, across a continuum of initial frequencies (Figure S7). While the initial frequency affects the proportion of all outcomes, it affects mainly the proportion of gene drive designs allowing gene swamping (blue curves in Figure S7). When considering only evolutionary dynamics, a higher initial frequency allows differential targeting with higher values of s.[6] In a single-population model[14] and in a two-population model,[6] for given values of s, c, and h, we can derive the threshold value of $q(0)$ above which the gene drive will spread from the equilibria of q.[14] Our results indicate that these gene drive designs lead to gene swamping outcomes in a combined evolutionary-demographic model. While this result demonstrates the constraints of attaining gene swamping outcomes in terms of deployment costs, it also indicates that gene swamping is perhaps achievable even at lower initial frequencies (e.g., $q_1(0) < 0.5$; Figure S7).

Gene swamping is more robust to spillover than suppression

So far, we have shown that migration rates influence the proportion of outcomes, and that certain suppression outcomes are

achievable only at low migration rates (Figure 2). An important aspect of gene drive design is robustness to variability that may be present in the ecosystem, such as changing migration rates or demography, or inability to accurately estimate these parameters. In order to compare the outcomes we identified in terms of their sensitivity to an increase in migration rates, we consider gene drives with a range of relative fitness costs s with a fixed conversion rate of $c = 1$ (i.e., no heterozygotes) for different values of m.

When m is sufficiently low, it is possible to design gene drives that achieve either suppression or gene swamping (bottom part of Figure 3A). Increasing the migration rate reduces the proportion of suppression and gene swamping outcomes (Figure 3A), as demonstrated in Figure 2B. These outcomes, for the same parameters other than m, are replaced by the spillover & collapse or failure outcomes. However, the gene drive design (in this case, the value of s) also influences whether an increase in migration will result in spillover & collapse (orange in Figure 3) or failure (purple in Figure 3). To illustrate this point, we consider three different designs ($s = 0.57$, 0.63, and 0.7), plotted as white dashed lines in Figure 3A. The first design ($s = 0.57$) achieves suppression at low migration rates, whereas the second and third designs ($s = 0.63$ and $s = 0.7$) lead to gene swamping. Increasing the migration rate shifts the first and second designs to spillover & collapse, at different thresholds of migration. However, the third design shifts to failure when increasing the migration rate. This demonstrates that some gene drive designs that lead to gene swamping will not lead to spillover & collapse if

A

B

Spillover
Spillover & Collapse
Differential targeting
Suppression
Oscillations
Gene swamping
Failure
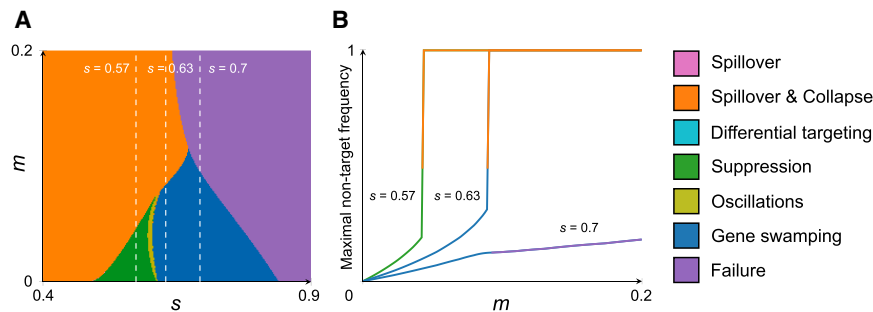
Figure 3. Designing gene drives to achieve "gene swamping" at low migration rates and failure at high migration rates

(A) Outcomes for different relative fitness costs (s) for increasing migration rates (m).

(B) Maximal non-target frequency (i.e., highest gene drive allele frequency in non-target population) for increasing levels of migration. Other parameters used for both panels are $c = 1$, $h = 1$, $q_1(0) = 0.8$, $d = 10$, and $r_0 = 2$.

migration rates increase. This feature, if incorporated into the design of the gene drive, could serve as a fail-safe, allowing deployment to accommodate variability in migration rate or imprecision in evaluation of migration rates, without the expected risk that the gene drive will spread to both populations.

An additional aspect to gene drive deployment is the effect of the gene drive on non-target populations[6]; in our model, this can be measured as the gene drive frequency in the non-target population in outcomes where it is present there at low frequencies (suppression, oscillations, and gene swamping). This reflects not only the increased risk of spread of the gene drive in the non-target population but also the risk of demographic effects on this population and further spread of the gene drive to other non-target populations through gene flow. For the three designs used above ($s = 0.57, 0.63,$ and 0.7), we also analyze the effect of deployment on the non-target population, defined as the maximal gene drive allele frequency in the non-target population during deployment, which we term the "maximal non-target frequency." We plotted the maximal non-target frequency for these designs for increasing migration rates, with the line color indicating the deployment outcome for this migration rate (i.e., change in line color indicates a shift in outcome at a threshold level of m in Figure 3B). For the first two designs that result in spillover & collapse in Figure 3A ($s = 0.57$ and $s = 0.63$), the maximal non-target frequency is high even below the threshold of m at which the outcome shifts to spillover & collapse (Figure 3B). In other words, the effect on the non-target population may be substantial even if no spillover occurs. For the third design in Figure 3A ($s = 0.7$), which does not result in the spillover & collapse outcome at any value of m, the maximal non-target frequency increases with m but is lower than that of the other two designs.

Suppression characteristics in gene swamping outcomes

As opposed to long-term suppression, in the gene swamping outcome, the gene drive is removed from both populations following a short-term targeted suppression phase (Figure 1D). The feasibility of gene drives allowing short-term suppression would depend on the effectiveness of the suppression phase. In order to characterize how gene drive design and migration affect the degree of suppression in this outcome, we studied three characteristics of the suppression phase (Figure 4A): (1) the duration (in generations) for which the target population is suppressed, (2) the maximal level, in terms of population size

or density, to which the population is suppressed, and (3) the total suppression of the target population during deployment (see Figure 4 for definition of these characteristics).

For gene drive designs achieving gene swamping, a higher relative fitness cost s results in less effective suppression; however, this mainly affects the duration of suppression, with the maximal suppression level decreasing only toward the end of the range of s values (Figures 4B–4D). In other words, with higher values of s, the targeted population collapses faster, shortening the suppression phase (Figure 4B). This relationship is consistent for different migration rates, with higher migration rates reducing both the duration and level of suppression (Figure S8).

Gene swamping is robust to the evolution of resistance

One of the main challenges in gene drive deployment is to reduce the possibility of evolution of resistance to the gene drive.[23,24,28,29] Resistance alleles can prevent fixation of the gene drive allele and even lead to its loss by competition with the gene drive allele. Resistance can arise through mutation of the wild-type allele targeted by the gene drive, in the same locus, interfering with the CRISPR targeting mechanism,[13,30] or through mutation of other loci that reduce conversion efficacy.[23] The emergence and spread of resistance alleles have long-term implications, because the persistence of a resistance allele after deployment increases the chance that future deployments of the same gene drive will fail.

To evaluate the probability of resistance evolving in our model, we integrated an evolutionary model of gene drive resistance[24] into the genetic element of our model (see method details section). We modeled two mechanisms through which resistance alleles are generated, *de novo* mutations of wild-type alleles (generated at a fixed rate μ) and non-homologous end-joining (NHEJ) events during gene drive conversion (generated at a fixed rate δ). In the *de novo* mutation case, the probability that a resistance allele will appear is correlated with the number of wild-type alleles in both populations, because only wild-type alleles can be converted to resistance alleles. In NHEJ-generated resistance alleles, this probability is correlated with the number of heterozygotes, because NHEJ events occur during conversion, which occurs only in heterozygotes. The spread of the resistance allele, once it has appeared, depends on the presence of the gene drive allele, because otherwise the resistance allele has no fitness advantage over the wild-type allele. Therefore, when considering the dynamics in the gene swamping outcome (Figure 1D), we expect
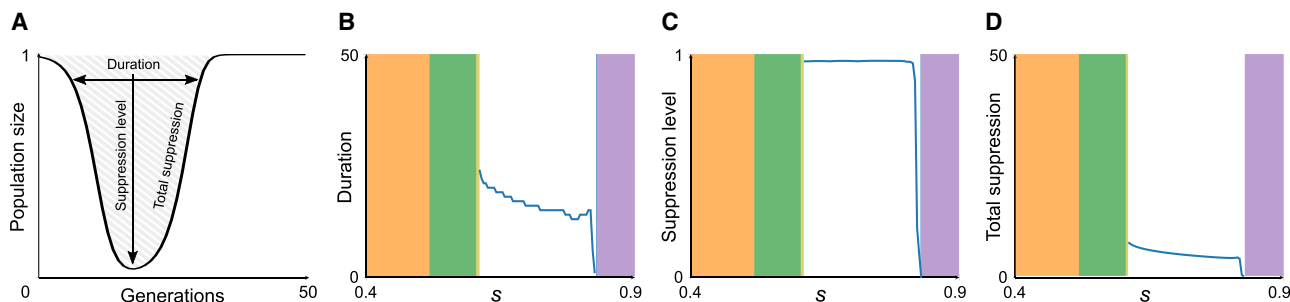
Figure 4. Characteristics of the "gene swamping" outcome

(A) Schematic representation of the characteristics studied: "suppression level" is the maximal proportion of the target population suppressed, "duration" is the number of generations for which the target population size is below the threshold level $N < 0.9K$, and "total suppression" is the accumulative suppression (area of the gray zone above the curve).

(B–D) Analysis of characteristics of suppression in gene swamping outcome for different gene drive designs (different values of s with a fixed conversion rate $c = 1$). Blue curves indicate the value of each parameter for gene swamping outcomes; values of s leading to other outcomes are colored according to the color legends in Figures 2 and 3. (B) The number of generations in which the target population is suppressed ("duration"). (C) The maximal suppression level. (D) The total suppression during gene swamping. In all panels the parameters used are $c = 1$, $h = 1$, $m = 0.01$, $q_1(0) = 0.8$, $d = 10$, and $r_0 = 2$. See also Figure S8.

that the duration of the suppression phase with different parameters (Figure 4B) will affect the probability of resistance evolving.

In Figure 5, we compare the probabilities that resistance does not evolve in the gene swamping and suppression outcomes with two different population sizes. These probabilities were computed using stochastic simulations, where we simulated resistance alleles generated by two different mechanisms, following the equations described in Unckless et al.[24] (see method details). To test the robustness of the suppression and gene swamping outcomes to the evolution of resistance, we chose gene drive design and migration parameters that result in either of these outcomes based on previous analyses of the model, and we ran simulations in which *de novo* mutations or NHEJ events occur stochastically. The outcome of these simulations will either be the "intended outcome" of suppression or gene swamping, or an establishment of the resistance allele and loss of the gene drive. We considered the robustness of an outcome to the evolution of resistance as the proportion of simulation runs in which resistance did not evolve. Since we were interested in the long-term effects of resistance evolution, we considered resistance to have evolved in simulations in which the resistance allele frequency was ≥ 0.1 at the end of the simulation (after 100 generations).

For resistance alleles generated through *de novo* mutations, we observe that gene swamping is more robust than suppression (i.e., fewer simulations resulted in significant spread of a resistance allele), and in both outcomes, the probability for resistance evolution does not depend on the migration rate (Figure 5A). With a larger population size ($K = 10,000$), the probability of resistance evolving is increased for suppression outcomes but not for gene swamping outcomes (Figure 5A). For resistance alleles generated through NHEJ events, the difference between the two outcomes is migration dependent (Figure 5B): at low levels of migration, both outcomes have a similar likelihood for resistance to evolve, while at higher levels of migration, gene swamping is more robust to the evolution of resistance than suppression (Figure 5B). For the larger population size that we simulated ($K = 10,000$), both outcomes have a higher likelihood of

resistance evolving at low migration rates. This is owing to the longer duration of suppression at low migration rates in gene swamping outcomes, leading to a longer window to allow the evolution of resistance.

The difference between the resistance-allele-generating mechanisms, in terms of the effect of migration, relates to the conditions that increase the likelihood of resistance alleles appearing. For *de novo* mutations, the rate of emergence of resistance alleles is a function of the number of wild-type alleles in the system (Equation 10). Therefore, the suppression of the target population is not sufficient to prevent the evolution of resistance, because *de novo* mutations can appear in the non-target population and spread to the target population through gene flow. For NHEJ events, emergence of resistance is a function of the number of heterozygotes in the system (Equation 11). For suppression outcomes, higher gene flow results in more intermediate levels of q in both populations (i.e., with higher m, q_1 is decreased and q_2 is increased) and, therefore, a higher proportion of heterozygotes in the system. In gene swamping outcomes, higher gene flow likewise increases the maximal non-target frequency (Figure 3B), increasing the frequency of heterozygotes during the suppression phase. This increases the likelihood of resistance evolving in both suppression and gene swamping outcomes but particularly for suppression due to the persistence of the gene drive allele in the system.

DISCUSSION

Gene drives have the potential to revolutionize biocontrol, but developing safe deployment approaches is crucial to avoiding unintentional spillover of the gene drive to non-target populations. Feedback between the evolutionary spread of the gene drive and its demographic effects may lead to non-optimal deployment outcomes, such as persistence of the gene drive, while preventing elimination of the target population.[9,25] Here, we show that this feedback can potentially result in gene drives that avoid spillover and persistence of the drive allele while still generating strong short-term suppression of the target

A *De novo* mutation   **B** NHEJ
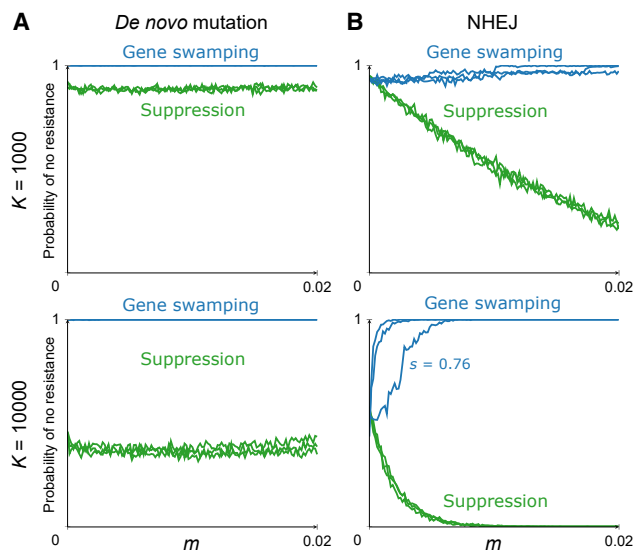
Figure 5. Evolution of resistance in gene swamping and suppression outcomes

Resistance alleles are generated either by *de novo* mutation (A) or non-homologous end-joining (NHEJ) during conversion (B). Plotted are the proportions of simulations for specific gene drive designs, across a range of migration rates, in which resistance did not evolve (see method details for detail of simulations), for two different population sizes (defined by K). Each line represents a specific gene drive design with the outcome in the absence of the evolution of resistance indicated by the color of the line: blue lines relate to values of s that lead to gene swamping outcomes ($s = 0.76$, $s = 0.8$, and $s = 0.84$); green lines relate values of s that lead to suppression outcomes ($s = 0.7$, $s = 0.71$, and $s = 0.72$). Other parameters used: $h = 0.75$, $c = 1$, $q_1(0) = 0.8$, $d = 10$, $r_0 = 2$, $\mu = 10^{-6}$ (A), and $\delta = 10^{-4}$ (B).

population without suppression of the non-target population (the "gene swamping" outcome).

Previous models of gene drive spread have taken either a purely soft selection approach,[6,15] in which the gene drive and wild-type alleles compete directly, or a hard selection approach, in which the demographic effect of the gene drive determines selection of the gene drive allele.[9,18,25] Our model combines these approaches, allowing us to analyze the effect of demographic feedback on deployment outcomes. This feedback, under some conditions, can generate outcomes of gene drive deployment that are absent when considering only evolutionary dynamics (Figure 1).

One of the main challenges in gene drive deployment is the containment of the released drive to a specific population. This issue is being addressed by the development of more complex gene drive architectures[20,22]; without these additional genetic safeguards, most gene drive designs are expected to either fail to spread or to result in uncontrolled spread of the gene drive even at low migration rates[5] (e.g., Figure 1A). Only a limited set of gene drive designs are expected to allow differential targeting of the gene drive at low migration rates[6] (Figures 1B and 1C). Our results, as well as results from continuous-space and reaction-diffusion models,[9,18] indicate that when targeted suppression is attempted in the presence of migration, local collapse of a target population or region results in either temporary or persis-

tent suppression and not in elimination of the populations. In such cases, demographic (Figure 1C) or spatial[25] oscillations resulting from demographic rescue or gene swamping are a possibility.

We focused our detailed analysis on the "gene swamping" outcome because its characteristics suggest that it could be used as a fail-safe for gene drive deployment. In this scenario, a temporary phase of suppression of the target population is followed by removal of the gene drive from both populations due to wild-type-abundant gene flow from the non-target population (Figure 1F). This outcome has several interesting features. (1) In terms of the range of gene drive designs and migration rates leading to this outcome, in comparison to long-term suppression of the target population, the gene swamping outcome is more robust to spillover (Figure 3A). (2) The gene swamping outcome is also more robust to the evolution of resistance (Figure 5). Short-term suppression decreases the chance of resistance evolving during deployment, whereas long-term persistence of the gene drive in the wild increases the probability that resistance to the gene drive will evolve. This may affect the potential for future deployment programs in the same population. (3) In the gene swamping outcome, at the end of the process, the gene drive allele is absent from both populations, but unlike in the "failure" outcome, a targeted suppression phase does occur. While this outcome offers only a confined window of suppression (Figure 4), non-genetic means of population suppression could be used during this window to achieve eradication of the target population. However, as opposed to long-term suppression, in the case that eradication is not achieved, the deployment will not result in spillover nor in the gene drive allele remaining in the system. Since these non-genetic control measures should be timed to coincide with the decrease in the size of the target population, control measures that are efficient at low population densities, such as mating disruption strategies (e.g., false pheromones), should be preferred over measures such as pesticides or sterile males.[31]

The investigation of gene drive deployment strategies has progressed mainly using mathematical and computational modeling. However, for the conclusions from these modeling efforts to be incorporated into upcoming gene drive projects, it is likely that experimental validation in a lab setting would be required. So far, experimental setups for population suppression using gene drives have been conducted using single caged populations[32] (usually with several replicates). In order to demonstrate the potential for spillover mitigation with different gene drive configurations, it would be important to design an experimental setup that includes population structure and that strongly relates to the setup of theoretical models. In this aspect, the modeling approach of two interconnected populations, as we have used here, is perhaps more readily translatable to an experimental setup, for example using two interconnected cages, compared to continuous-space models.

Our model demonstrates the importance of considering the interaction between the evolutionary and demographic effects of gene drives. With such feedback, qualitatively different outcomes may emerge, which may have implications for designing gene drive configurations and deployment strategies. In our model, asymmetrical gene flow caused by changes in relative

population size between target and non-target populations was shown to generate an outcome of interest that we termed "gene swamping." This fail-safe strategy does not rely on the complexity of the gene drive construct[19,20,22,33] but rather on gene flow and population dynamics. Since these aspects are general features of wild populations, this approach could be readily combined with other types of fail-safe mechanisms to prevent the unintended spread of gene drive constructs.

Limitations of the study

Our models are designed to identify novel outcomes of gene drive deployment that could be generated by feedbacks between evolutionary and demographic dynamics during gene drive spread. Our results support the importance of considering feedbacks between evolution and demography. Our models are not intended for quantitatively assessing gene drive parameters and evaluating specific deployment programs. Such system-specific parameterization would require a far more detailed model and consideration of many ecological factors not included here.[8]

STAR★METHODS

Detailed methods are provided in the online version of this paper and include the following:

- KEY RESOURCES TABLE
- RESOURCE AVAILABILITY
  - Lead contact
  - Materials availability
  - Data and code availability
- METHOD DETAILS
  - Migration between populations
  - Soft selection and conversion
  - Demographic dynamics
  - Demographic effect of the gene drive
  - Population dynamics
  - Classification of outcomes
  - Evolution of resistance
- ADDITIONAL RESOURCES

SUPPLEMENTAL INFORMATION

Supplemental information can be found online at https://doi.org/10.1016/j.celrep.2023.113499.

AUTHOR CONTRIBUTIONS

K.D.H. and G.G. developed the model. K.D.H. analyzed the model and generated figures. K.D.H. and G.G. co-authored the manuscript. G.G. supervised and acquired funding for the research.

REFERENCES

1. Alphey, L.S., Crisanti, A., Randazzo, F.F., and Akbari, O.S. (2020). Opinion: Standardizing the definition of gene drive. Proc. Natl. Acad. Sci. USA 117, 30864–30867.

2. Gantz, V.M., Jasinskiene, N., Tatarenkova, O., Fazekas, A., Macias, V.M., Bier, E., and James, A.A. (2015). Highly efficient Cas9-mediated gene drive for population modification of the malaria vector mosquito Anopheles stephensi. Proceedings of the National Academy of Sciences. Proc. Natl. Acad. Sci. USA 112, E6736–E6743.

3. Hammond, A., Galizi, R., Kyrou, K., Simoni, A., Siniscalchi, C., Katsanos, D., Gribble, M., Baker, D., Marois, E., Russell, S., et al. (2016). A CRISPR-Cas9 gene drive system targeting female reproduction in the malaria mosquito vector Anopheles gambiae. Nature Biotechnology. Nat. Biotechnol. 34, 78–83.

4. Bier, E. (2022). Gene drives gaining speed. Nat. Rev. Genet. 23, 5–22.

5. Noble, C., Adlam, B., Church, G.M., Esvelt, K.M., and Nowak, M.A. (2018). Current CRISPR gene drive systems are likely to be highly invasive in wild populations. Elife 7, e33423.

6. Greenbaum, G., Feldman, M.W., Rosenberg, N.A., and Kim, J. (2021). Designing gene drives to limit spillover to non-target populations. PLoS Genet. 17, e1009278.

7. Price, T.A.R., Windbichler, N., Unckless, R.L., Sutter, A., Runge, J.N., Ross, P.A., Pomiankowski, A., Nuckolls, N.L., Montchamp-Moreau, C., Mideo, N., et al. (2020). Resistance to natural and synthetic gene drive systems. J. Evol. Biol. 33, 1345–1360.

8. Kim, J., Harris, K.D., Kim, I.K., Shemesh, S., Messer, P.W., and Greenbaum, G. (2023). Incorporating ecology into gene drive modelling. Ecol. Lett. 26, S62–S80.

9. Girardin, L., and Débarre, F. (2021). Demographic feedbacks can hamper the spatial spread of a gene drive. J. Math. Biol. 83, 67.

10. James, S., Collins, F.H., Welkhoff, P.A., Emerson, C., Godfray, H.C.J., Gottlieb, M., Greenwood, B., Lindsay, S.W., Mbogo, C.M., Okumu, F.O., et al. (2018). Pathway to deployment of gene drive mosquitoes as a potential biocontrol tool for elimination of malaria in sub-Saharan Africa: recommendations of a scientific working group. Am. J. Trop. Med. Hyg. 98, 1–49.

11. James, S.L., Marshall, J.M., Christophides, G.K., Okumu, F.O., and Nolan, T. (2020). Toward the definition of efficacy and safety criteria for advancing gene drive-modified mosquitoes to field testing. Vector Borne Zoonotic Dis. 20, 237–251.

12. Hartl, D.L. (1970). Analysis of a general population genetic model of meiotic drive. Evolution 24, 538–545.

13. Burt, A. (2003). Site-specific selfish genes as tools for the control and genetic engineering of natural populations. Proc. Biol. Sci. 270, 921–928.

14. Deredec, A., Burt, A., and Godfray, H.C.J. (2008). The population genetics of using homing endonuclease genes in vector and pest management. Genetics 179, 2013–2026.

15. Unckless, R.L., Messer, P.W., Connallon, T., and Clark, A.G. (2015). Modeling the manipulation of natural populations by the mutagenic chain reaction. Genetics 201, 425–431.

16. Verma, P., Reeves, R.G., and Gokhale, C.S. (2021). A common gene drive language eases regulatory process and eco-evolutionary extensions. BMC Ecology and Evolution. BMC Ecol. Evol. 21, 156.

17. Tanaka, H., Stone, H.A., and Nelson, D.R. (2017). Spatial gene drives and pushed genetic waves. Proc. Natl. Acad. Sci. USA *114*, 8452–8457.

18. Champer, J., Zhao, J., Champer, S.E., Liu, J., and Messer, P.W. (2020). Population dynamics of underdominance gene drive systems in continuous space. ACS Synth. Biol. *9*, 779–792.

19. Sudweeks, J., Hollingsworth, B., Blondel, D.V., Campbell, K.J., Dhole, S., Eisemann, J.D., Edwards, O., Godwin, J., Howald, G.R., Oh, K.P., et al. (2019). Locally fixed alleles: a method to localize gene drive to island populations. Sci. Rep. *9*, 15821.

20. Noble, C., Min, J., Olejarz, J., Buchthal, J., Chavez, A., Smidler, A.L., DeBenedictis, E.A., Church, G.M., Nowak, M.A., and Esvelt, K.M. (2019). Daisy-chain gene drives for the alteration of local populations. Proc. Natl. Acad. Sci. USA *116*, 8275–8282.

21. Li, M., Yang, T., Kandul, N.P., Bui, M., Gamez, S., Raban, R., Bennett, J., Sánchez C, H.M., Lanzaro, G.C., Schmidt, H., et al. (2020). Development of a confinable gene drive system in the human disease vector Aedes aegypti. Elife *9*, e51701.

22. Terradas, G., Buchman, A.B., Bennett, J.B., Shriner, I., Marshall, J.M., Akbari, O.S., and Bier, E. (2021). Inherently confinable split-drive systems in Drosophila. Nat. Commun. *12*, 1480.

23. Gomulkiewicz, R., Thies, M.L., and Bull, J.J. (2021). Evading resistance to gene drives. Genetics *217*, iyaa040.

24. Unckless, R.L., Clark, A.G., and Messer, P.W. (2017). Evolution of resistance against CRISPR/Cas9 gene drive. Genetics *205*, 827–841.

25. Champer, J., Kim, I.K., Champer, S.E., Clark, A.G., and Messer, P.W. (2021). Suppression gene drive in continuous space can result in unstable persistence of both drive and wild-type alleles. Mol. Ecol. *30*, 1086–1101.

26. Haldane, J.B.S. (1956). The relation between density regulation and natural selection. Proc. R. Soc. Lond. B Biol. Sci. *145*, 306–308.

27. Thomé, R.C.A., Yang, H.M., and Esteva, L. (2010). Optimal control of *Aedes aegypti* mosquitoes by the sterile insect technique and insecticide. Math. Biosci. *223*, 12–23.

28. Marshall, J.M., Buchman, A., Sánchez C, H.M., and Akbari, O.S. (2017). Overcoming evolved resistance to population-suppressing homing-based gene drives. Sci. Rep. *7*, 1–12.

29. Prowse, T.A.A., Cassey, P., Ross, J.V., Pfitzner, C., Wittmann, T.A., and Thomas, P. (2017). Dodging silver bullets: good CRISPR gene-drive design is critical for eradicating exotic vertebrates. Proc. Biol. Sci. *284*, 20170799.

30. Champer, J., Reeves, R., Oh, S.Y., Liu, C., Liu, J., Clark, A.G., and Messer, P.W. (2017). Novel CRISPR/Cas9 gene drive constructs reveal insights into mechanisms of resistance allele formation and drive efficiency in genetically diverse populations. PLoS Genet. *13*, e1006796.

31. Lampert, A., and Liebhold, A.M. (2021). Combining multiple tactics over time for cost-effective eradication of invading insect populations. Ecol. Lett. *24*, 279–287.

32. Hammond, A., Pollegioni, P., Persampieri, T., North, A., Minuz, R., Trusso, A., Bucci, A., Kyrou, K., Morianou, I., Simoni, A., et al. (2021). Gene-drive suppression of mosquito populations in large cages as a bridge between lab and field. Nat. Commun. *12*. 4589–9.

33. Xu, X.-R.S., Bulger, E.A., Gantz, V.M., Klanseck, C., Heimler, S.R., Auradkar, A., Bennett, J.B., Miller, L.A., Leahy, S., Juste, S.S., et al. (2020). Active genetic neutralizing elements for halting or deleting gene drives. Mol. Cell. *80*, 246–262.e4.

34. Harris, K.D., Hadari, G., and Greenbaum, G. (2022). modelRxiv: A platform for the distribution, computation and interactive display of models. Preprint at bioRxiv. https://www.biorxiv.org/content/early/2022/02/19/2022.02.16.480599.full.pdf.

35. Beverton, R.J., and Holt, S.J. (1995). in Sea Fisheries. In Their Investigation in the United Kingdom, M. Graham, ed. (Edward Arnold), pp. 372–441.

36. Sedda, L., Taylor, B.M., Eiras, A.E., Marques, J.T., and Dillon, R.J. (2020). Using the intrinsic growth rate of the mosquito population improves spatio-temporal dengue risk estimation. Acta Trop. *208*, 105519.

STAR★METHODS

KEY RESOURCES TABLE

REAGENT or RESOURCE	SOURCE	IDENTIFIER
Software and algorithms		
modelRxiv	modelrxiv.org	doi: https://doi.org/10.1101/2022.02.16.480599
Model code	Zenodo	doi: https://doi.org/10.5281/zenodo.8004590

RESOURCE AVAILABILITY

Lead contact
Further information and requests for resources should be directed to and will be fulfilled by the lead contact, Gili Greenbaum (gil.g@mail.huji.ac.il)

Materials availability
This study is theoretical and did not generate new unique reagents.

Data and code availability
- Data. This theoretical study did not generate new data.
- Code. Model code is available on modelRxiv at the URLs noted above, GitHub (https://github.com/carrowkeel/genedrive_demographic) and Zenodo (https://doi.org/10.5281/zenodo.8004590).
- Any additional information required to reanalyze the results reported in this paper is available from the lead contact upon request.

METHOD DETAILS

To study gene drive dynamics and spillovers in the presence of feedback between the evolutionary dynamics and the demographic impact of the gene drive, we developed and investigated two-population mathematical models tracking the gene drive allele frequency and the population sizes. Our focus was to investigate conditions under which the gene drive is potentially able to spread to different frequencies in the two populations ("differential targeting" gene drives[6]). We limited our study to suppression gene drives,[4] in which the relative fitness cost of the gene drive allele can be manipulated to generate threshold-dependent[15] gene drives. Modification gene drives, the purpose of which is not to reduce the population size but to alter a trait of the organism (e.g., its transmission of diseases), are not expected to be threshold-dependent without additional genetic architecture limiting their spread[4]; we do not study such gene drives here.

Our model consists of two dynamics that are related to the spread of gene drives: (i) an evolutionary dynamic, tracking the change in the gene drive allele frequency q, and (ii) a demographic dynamic, tracking the impact of the gene drive on populations sizes N. In order to understand the impact of gene flow during gene drive spread, we model two populations, identical in terms of their carrying capacity, which are connected by migration. We formulate two sets of recursive equations, one set for tracking the gene drive allele frequency in the two populations q_i, and one set for tracking the two population sizes, N_i $(i = 1, 2)$. For simplicity and coherence, we define population 1 as the 'target population' that we aim to suppress and where the gene drive is deployed, and population 2 as the 'non-target population'. The model is implemented and available on the modelRxiv platform,[34] where all results can be regenerated and the model can be re-parameterized (https://modelrxiv.org/model/yoKkSv). The life cycle used in the model, along with a scheme of the model dynamics and feedbacks between them are illustrated in Figure S1. The parameters used for model analyses are indicated in Table S1.

Migration between populations
We consider the case where migration occurs prior to selection and population growth (Figure S1), which refer broadly to change in allele frequency due to the fitness cost of the gene drive, and change in population sizes due to the fitness cost of the gene drive. We model changes in population sizes in two steps: from pre-migration to post-migration, and then from post-migration to post-selection. We consider here only the migration-before-selection case because the results are typically similar in the selection-before-migration case.[6] For simplicity, we only consider the case where migration is inherently symmetric, with a proportion m of each

population migrating per generation (i.e., symmetric in terms of the proportion of migration, but may be asymmetric in terms of number of individuals migrating when the population sizes are unequal). We formulate the change in the population size of population i from the pre-migration sizes, denoted as N_i, to the post-migration sizes, denoted as $\tilde{N}_i$:

$$\tilde{N}_i = (1-m)N_i + mN_j. \quad \text{for } i,j = 1,2; i \neq j \qquad \text{(Equation 1)}$$

To model the impact of migration on the genetic composition of population i, we formulate the change from the pre-migration gene drive allele frequency in population i, denoted as q_i, to the post-migration frequency, denoted as $\tilde{q}_i$:

$$\tilde{q}_i = \left[(1-m)2N_i q_i + 2mN_j q_j\right]\frac{1}{2\tilde{N}_i}. \quad \text{for } i,j = 1,2; i \neq j \qquad \text{(Equation 2)}$$

In Equation 2, the number of gene drive alleles in the population following migration is normalized by the population size to compute the post-migration allele frequencies.

Soft selection and conversion

To model evolutionary dynamics, we use a previously studied model of gene drive dynamics in two populations,[6] which is based on a model of gene drive spread in a single diploid population.[14,15] This model considers the fitness cost of the gene drive allele (A) homozygote relative to the wild type allele (a), s, the dominance of the gene drive allele, h, and the conversion rate of heterozygotes (Aa) to gene drive homozygotes (AA) by the CRISPR copying mechanism, c. In our model we consider gametic conversion of the wild type allele (we present results for a zygotic conversion model in Note S4 in Data S1). The change in the gene drive allele frequency in population i from the post-migration frequencies $\tilde{q}_i$ (Equation 2) to the post-selection frequencies q'_i can be described by the recursion equation[6]

$$q'_i = \frac{\tilde{q}_i^2(1-s) + \tilde{q}_i(1-\tilde{q}_i)(1+c)(1-hs)}{\overline{w}_i}, \qquad \text{(Equation 3)}$$

where the average fitness $\overline{w}_i$ is defined as $\overline{w}_i = \tilde{q}_i^2(1-s) + 2\tilde{q}_i(1-\tilde{q}_i)(1-hs) + (1-\tilde{q}_i)^2$. In this model, migration occurs before random mating, followed by conversion and selection (Figure S1). While the life cycle may alter the outcome of the model for specific parameters, the overall effect of the order of events in the life cycle is expected to be minor.[6]

Demographic dynamics

To model demographic dynamics, we use the Beverton-Holt model[35] to describe changes in populations sizes following migration ($\tilde{N}_i$ in Equation 1):

$$N'_i = R_i \tilde{N}_i \frac{K}{K + (R_i - 1)\tilde{N}_i}, \qquad \text{(Equation 4)}$$

where K is the carrying capacity (assumed identical for both populations) and R_i is the growth rate of population i (for an alternative demographic model, see Note S3 in Data S1). We also consider the populations identical in terms of their intrinsic growth rates (i.e., the growth rate of the population without the gene drive allele and far from carrying capacity). As the growth rate is affected by the spread of the gene drive, we treat the actual growth rate of the populations as a dynamic parameter, R_i, which depends on the gene drive allele frequency. Instead of computing genotype frequencies separately using their respective growth rates (hard selection), we assume that the population has a single growth rate that is a function of its genotype frequencies. This allows us to separate between the effect of the gene drive on soft selection, for example intra-population competition that can alter the gene drive allele frequency (in the soft selection step above), and its effect on the overall growth or collapse of the population. To describe the relationship between the population growth rate and its genetic composition, we define "genotype growth rates", which are weights we use to compute the population growth rate based on the population's genetic composition. We denote the growth rate of a genotype with relative fitness cost s as $r_{(s)}$. Thus, the intrinsic growth rate in the absence of the gene drive is denoted r_0, and the intrinsic growth rate of a population fixed for the gene drive allele is $r_{(s)}$. For all analyses, we defined $r_0 = 2$, which means that the population at most doubles in every generation (e.g., mosquito populations[36]). The intrinsic population growth rate R_i at a given point in time is, therefore, computed by weighing the different growth rates with the post-selection genotype frequencies of the gene drive allele:

$$R_i = G'_{aa,i}r_0 + G'_{Aa,i}r_{(hs)} + G'_{AA,i}r_{(s)}, \qquad \text{(Equation 5)}$$

where $G'_{aa,i} = (1-\tilde{q}_i)^2$, $G'_{Aa,i} = 2\tilde{q}_i(1-\tilde{q}_i)(1-hs)$ and $G'_{AA,i} = \tilde{q}_i^2(1-s)$. Equation 5 links the demographic dynamics described in Equations 1 and 4 with the evolutionary dynamics of Equations 2 and 3, which together comprise the dynamical system we study.

Demographic effect of the gene drive

The function $r_{(s)}$ describes the demographic impact of the gene drive, and is related to the relative fitness cost s of the gene drive allele. This function is of particular interest, because it defines the population-level impact of the gene drive allele, and therefore could vary depending on the demographic effect of the gene drive phenotype on the population. If the gene drive has no demographic effect

(i.e., gene drive carriers have decreased intra-species competitive abilities, but do not suffer from absolute fitness costs), $r_{(s)}$ should be independent of s and equal to the intrinsic growth rate r_0. If the demographic effect is correlated to the effect of the gene drive on relative fitness, s and $r_{(s)}$ should be tightly linked. To model this relationship, we introduce a parameter d that allows the manipulation of the level of the demographic effect of the gene drive; this parameter determines the degree to which growth rate $r_{(s)}$ is impacted in relation to the relative fitness cost s of the genotype (e.g., for heterozygotes, we compute $r(hs)$ by substituting s with hs):

$$r_{(s)} = r_0 - (1 - e^{-ds})(s + r_0 - 1).$$ (Equation 6)

Under this formulation, for $d = 0$, the gene drive has no effect on growth rate (i.e., soft selection; $r_{(s)} = r_0$), whereas $d \to \infty$, we have $r_{(s)} \to 1 - s$, meaning that the population decline rate is fully correlated with the relative fitness cost. Intermediate values of d represent partial correlations between within-population competition and population-level demographic effects. The formulation in Equation 6 was chosen to allow the manipulation of the demographic effect of the gene drive and generate a continuum between the purely evolutionary dynamics and the demographic-evolutionary dynamics, and does not represent any particular relationship between genotypes and fitness. An alternative simplified formulation of $r_{(s)}$ does not substantially alter the outcome of the model (see Note S2 in Data S1).

Population dynamics
The population dynamics are governed by Equations 1 and 4. In Equation 4, when $\tilde{N}_i = K$ the population size would remain fixed from that point onward. To avoid the population size remaining fixed at K when we initialize the dynamics, we defined the initial population size of both populations as $N_i(0) = K(1 - \epsilon)$. We used $\epsilon = 0.01$ through all analyses. Changing the value of ϵ changes the delay of the demographic effect of the gene drive: lower values delay the demographic effect, while higher values increase the rate of the demographic effect.

Classification of outcomes
We classified the outcomes based on the evolutionary (Equation 3) and the demographic (Equation 4) dynamics. To differentiate between outcomes, we consider (i) the gene drive allele frequency and population size at $t = 100$, and (ii) the minimum population size. These definitions allows us to connect outcomes to functional aspects of deployment (e.g., the minimum population size is a measure of the effectiveness of suppression during deployment). For each outcome, we define thresholds of these two parameters. For example, we classify the outcome as 'suppression' when the target population has a high frequency (≥ 0.5) of the gene drive allele, the non-target population has a low frequency (< 0.5) of the gene drive allele, the target population is suppressed ($N_1 < 0.9K$, i.e., less than 90% of its initial size), and the non-target population was not suppressed ($\min(N_2) \geq 0.9K$). For 'oscillations', in addition to the thresholds in this table, we consider dynamics in which the target population size oscillates with an amplitude above a certain threshold (> 0.5). The full classification of outcomes is detailed in Table S2.

We defined three characteristics of the suppression phase in the target population (Figure 4A): (i) the duration of suppression, (ii) the maximal suppression level, and (iii) the total suppression. The duration of suppression was defined as the number of generations in which the target population size is suppressed ($N_1 < 0.9K$, i.e., less than 90% of its initial size). The maximal suppression level is defined as $\frac{\min(N_1)}{K}$. The total suppression is defined as $\sum_{i=1}^{n} 1 - \frac{N_1(t)}{K}$, where n is the total number of generations.

Evolution of resistance
In order to measure the effect of the evolution of resistance on the outcomes of our model, we modified the genetic element of the model, using a previous model [24] that considers three possible alleles at the gene drive locus: a (wild type allele), A (gene drive allele) and b (resistance allele). Here, in addition to the gene drive allele, we track the frequency of the resistance allele in the two populations, p_i. To account for gene flow of the resistance allele, we add an equation analogous to Equation 2 to compute the post-migration resistance allele frequency $\tilde{p}$:

$$\tilde{p}_i = \left[(1 - m)2N_ip_i + 2mN_jp_j\right]\frac{1}{2\tilde{N}_i}. \quad \text{for } i,j = 1,2; i \neq j$$ (Equation 7)

Because the resistance allele prevents conversion, we only need to account for conversion for A/a heterozygotes. We define s_b as the relative fitness cost of the resistance allele b. We assume that the resistance allele is codominant with the wild type allele, and that the dominance of the gene drive allele over the wild type allele, h, is equal to the dominance of the gene drive allele over the resistance allele. Using these parameters, we define the evolutionary dynamics in a similar manner as in Equation 3 for each population following Unckless et al.[24]:

$$q'_i = \frac{\tilde{q}_i^2(1 - s) + \tilde{q}_i(1 - \tilde{q}_i - \tilde{p}_i)(1+c)(1 - hs) + \tilde{q}_i\tilde{p}_i(1 - hs - (1 - h)s_b)}{\overline{w}_i}$$ (Equation 8)

$$p'_i = \frac{\tilde{p}_i^2(1 - s_b) + \tilde{p}_i(1 - \tilde{q}_i - \tilde{p}_i)(1 - s_b/2) + \tilde{p}_i\tilde{q}_i(1 - hs - (1 - h)s_b)}{\overline{w}_i}$$ (Equation 9)

These recurrence equations incorporate the gene drive design parameters (s, c and h) and the relative fitness cost and dominance of the resistance allele (s_r and h_r, respectively). Accounting for the resistance allele p_i, the mean fitness in the two populations is now

$$\overline{w}_i = \tilde{q}_i^2(1-s) + 2\tilde{q}_i\tilde{p}_i(1-hs-(1-h)s_b) + 2\tilde{q}_i(1-\tilde{q}_i-\tilde{p}_i)(1-hs) + 2\tilde{p}_i(1-\tilde{q}_i-\tilde{p}_i)(1-s_b/2) + \tilde{p}_i^2(1-s_b) + (1-\tilde{q}_i-\tilde{p}_i)^2.$$

For the purpose of investigating the likelihood of resistance establishing in the population we are mainly interested in the emergence of a significant level of resistance alleles in either population, and not in the loss of resistance alleles following the loss of the gene drive allele (through competition with the wild type allele). Therefore, we set the relative fitness cost of the resistance allele to $s_b = 0$. This implies that, in our analysis, the frequency of resistance alleles will remain at a fixed level once the gene drive allele is lost because it has no disadvantage relative to the wild type allele. This assumption is useful for the evaluation of the maximal spread of the resistance allele under different conditions.

Because we assume the relative fitness of the wild type allele a and resistance allele b is the same, we can replace $G'_{aa,i} = G'_{aa,i} + G'_{ab,i} + G'_{bb,i}$, and $G'_{Aa,i} = G'_{Aa,i} + G'_{Ab,i}$ in Equation 5 to compute the growth rates in the presence of the resistance allele.

We considered two mechanisms through which resistance alleles are generated[24]: *de novo* mutations of the wild type allele to a resistance allele that cannot be converted, and non-homologous end-joining during conversion resulting in a resistance allele (as opposed to a converted gene drive allele). *De novo* mutations appear as a function of population size and wild type alleles[24]:

$$u_\mu = 2\tilde{N}_i\mu\left[(1-\tilde{q}_i)^2 + \tilde{q}_i(1-\tilde{q}_i)(1-c)\right], \tag{Equation 10}$$

where u_μ is the *de novo* mutation rate, and $\tilde{N}_i$ is the population size after migration. For our simulations, we define $\mu = 10^{-6}$. The factors $(1-\tilde{q}_i)^2$ and $\tilde{q}_i(1-\tilde{q}_i)(1-c)$ are the proportions of wild type homozygotes and half the non-converted heterozygotes, respectively.

In the case of NHEJ, events occur as a function of population size and gene drive/wild type heterozygotes[24]:

$$u_\delta = 2\tilde{N}_i\delta c\tilde{q}_i(1-\tilde{q}_i), \tag{Equation 11}$$

where u_δ is the rate of NHEJ events, and $\tilde{N}_i$ is the population size after migration. For our simulations, we define $\delta = 10^{-4}$. $c\tilde{q}_i(1-\tilde{q}_i)$ is the proportion of converted heterozygotes. In each generation, the number of resistance alleles is drawn from a Poisson distribution with rate given by either u_μ or u_δ.

To compute the probability of resistance evolving either through *de novo* mutation or NHEJ events, we chose gene drive design and migration parameters that result in either the suppression or gene swamping outcomes based on previous analyses of the model, and ran stochastic simulations with the two resistance allele generating mechanisms. The outcome of these simulations will either be the 'intended outcome' of suppression or gene swamping, or the evolution of resistance and loss of the gene drive. For each simulation run, we defined the evolution of resistance according to the resistance allele frequency p after 100 generations, where $p \geq 0.1$ was considered as resistance having evolved. We ran 1000 simulation repeats for different gene drive designs (different values of s) for different population sizes, defined by the carrying capacity K, within a range of migration rates m. We considered the proportion of simulations for a given parameter set in which resistance did not evolve as the robustness to the evolution of resistance for the 'intended outcome' of these parameters.

ADDITIONAL RESOURCES

To facilitate further exploration of our results, we uploaded the model code to the platform modelRxiv, which allows visualization and analysis of models through a simple user interface (Harris et al.[34]; https://modelrxiv.org/model/yoKkSv for JavaScript model and https://modelrxiv.org/model/FPDRyL for Python model). In this platform, the results can be regenerated and the model can be re-parameterized (Figure S9).